

Femtosecond Laser Slicing of Single Crystal AlN Layer Grown by Hydride Vapor Phase Epitaxy on an AlN Substrate Generated by Physical Vapor Transport

Yang Yang¹, Katsuo Matsui¹, Yasuhiko Shimotsu^{*1}, Taishi Furuya², Reo Yamamoto², Toru Nagashima², Masahiro Shimizu¹, and Kiyotaka Miura¹

¹Department of Material Chemistry, Graduate School of Engineering,
Kyoto University, Kyoto 615-8510, Japan

²Tsukuba Research Laboratories, Tokuyama Corporation, Tsukuba, Ibaraki 300-4247, Japan

^{*}Corresponding author's e-mail: Shimotsu.yasuhiko.3m@kyoto-u.ac.jp

Aluminum nitride (AlN) is one of the highly anticipated materials for deep-ultraviolet (UV) optoelectronic devices due to its wide-bandgap and high thermal conductivity. Growing a thick single-crystal AlN layer by Hydride Vapor Phase Epitaxy (HVPE) method on another AlN substrate generated by Physical Vapor Transport (PVT) method is an effective method to obtain pure single crystal AlN. However, the waste of PVT-AlN is a serious obstruct for industrialization. In this study, the laser slicing of HVPE-AlN and PVT-AlN by femtosecond laser pulses was performed. The surface roughness of the separated HVPE-AlN was smaller than 120 μ m, while the separated PVT-AlN substrate was successfully used to grown a new single crystal AlN by HVPE after polishing. Femtosecond laser double spots scanning by using a SLM was also investigated to improve the efficiency.

DOI: 10.2961/jlmn.2024.01.2010

Keywords: ultrashort pulse laser processing, aluminum nitride, kerf loss, reuse of substrate, double spot laser slicing

1. Introduction

Aluminum nitride (AlN) is a direct band gap semiconductor with a wide-bandgap (~ 6.0 eV) and a high thermal conductivity (~ 268 to 374 W/m·K) [1,2]. Thanks to these properties, AlN, especially the single-crystal AlN with low dislocation density, is one of the highly anticipated materials for deep-ultraviolet (UV) optoelectronic devices which have great potential for the application in sterilization and virus inactivation [3-8].

Due to the high melting point ($\sim 2200^\circ\text{C}$) of AlN, it is hard to grow bulk AlN crystal from melt. The main growth methods of bulk AlN crystal include physical vapor transport (PVT) method and hydride vapor phase epitaxy (HVPE) method. A recent study has combined these two methods, growing a thick single-crystal AlN layer by HVPE method on another PVT-AlN substrate, to achieve higher purity and higher deep-UV optical transparency [9]. The HVPE-AlN was water-clear and free of stress and cracks, while the PVT-AlN substrate was amber in color with the presence of Al vacancies, substitutional impurities, and their complexes. In the previous study [9], the PVT-AlN substrate was removed by polishing, resulting in the waste of the substrates. To efficiently obtain the HVPE-AlN and reuse the PVT-AlN substrate, femtosecond laser slicing is one of the effective methods due to the extremely high-power density and high spatial resolution [10].

In this study, the laser slicing of HVPE-AlN and PVT-AlN by femtosecond laser pulses is performed. In particular, the interaction between femtosecond laser and materials at the interface of two layers of AlN is revealed and the laser slicing by multiple spots is investigated. We also

demonstrate that the PVT-AlN substrate after separation is able to be reused to grow a new HVPE-AlN.

2. Experiments

In the experiments, we used the samples made from Tokuyama Corporation with a thickness of 1 mm (400 μ m PVT-AlN and 600 μ m HVPE-AlN). The samples were cut into 5×5 mm and 2×5 mm. The schematic of the experiments is shown in Fig. 1(a). The femtosecond laser we used was Ti:sapphire laser centered at 800 nm. The pulse duration and the repetition rate were 120 fs and 1 kHz, respectively. The laser pulses were focused at the interface of the sample from HVPE side to PVT side by a $50\times$ objective (Nikon, NA=0.8). A spatial light modulator (LCOS-SLM, X10468-02, Hamamatsu Photonics K.K.) was used to compensate the spherical aberration. After the laser pulses were scanned through the whole interface of the sample, the sample was completely separated into two pieces by a Universal Testing System (Model 1122, Instron), which was shown in Fig. 1(b). A blade was put perpendicular to the sample to support the separation process. The surface roughness of the separated samples was measured by a surface profiler (Dektak150 BRUKER).

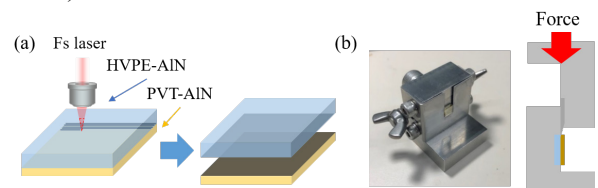


Fig. 1 (a) The schematic of the femtosecond laser scanning. (b) The equipment and schematic of the separation after scanning.

3. Results and discussions

3.1 Laser damage threshold

It is known that the cross-section of multiphoton ionization in dielectric material was associated with the polarization state when irradiated by femtosecond laser, resulting in the polarization sensitive femtosecond laser damage threshold [11]. Here we measured the femtosecond laser damage threshold at different depth with circular polarized (CP) pulses and linear polarized (LP) pulses. It was difficult to measure the focus spot size in the interface of the sample, so we used the single pulse energy on the sample surface here to compare the behaviors of LP pulses and CP pulses. As shown in Fig. 2, under our experiment condition, due to the spherical aberration and nonlinear processing, the threshold was raised with the increase of focusing depth expect for the interface. The lowest threshold was at the interface. This is primarily because of the unstable structure around the interface which induced by the lattice mismatch of HVPE-AIN and PVT-AIN. In addition, the threshold of LP pulses was always lower than that of CP pulses. The behavior can be explained by the linear-polarization dominance of multiphoton ionization cross section when N is large, where N is the order of the multiphoton ionization [12]. The lowest femtosecond laser damage threshold was found at the interface, which was about 580 nJ for CP pulses and 315 nJ for LP pulses. According to our results, the LP pulses was chosen to be focused at the interface of the sample for the reduction of material cost.

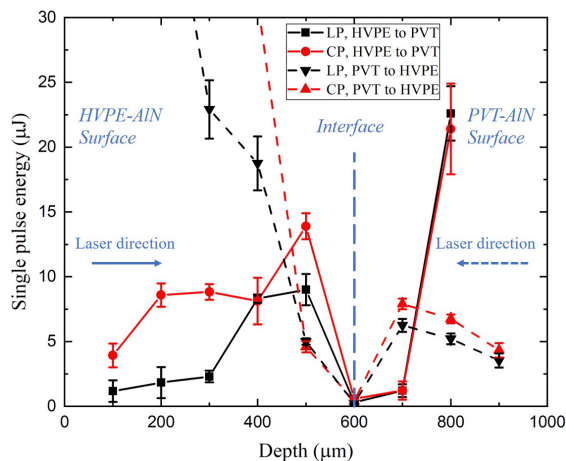


Fig. 2 The dependence of the laser damage threshold on depth for CP and LP pulses. The surfaces of HVPE-AIN and PVT-AIN were at 0 and 1000 μm respectively. The interface was at around 600 μm . The solid and dashed lines represented the laser irradiated direction from HVPE-AIN to PVT-AIN and from PVT-AIN to HVPE-AIN.

3.2 Parameters affecting femtosecond laser slicing

To optimize the laser slicing condition, several experimental parameters were investigated, including pulse energy, scanning speed, and laser polarization.

Pulse energy is always an important factor in femtosecond laser-matter interaction because it determines the regime of laser modification [13]. For the purpose of slicing, the regime of modification should be voids and cracks, which are resulting from the plasma explosion caused by high intensity [14]. Figure 3(a) shows the scanning lines induced by femtosecond laser pulses with different pulse energy at the scanning speed of 100 $\mu\text{m/s}$. When the pulse

energy was too low, the regime of laser modification dropped into anisotropic nanostructure with birefringence [15] which could not provide enough damage for separation. However, when the pulse energy was too high, the cracks were generated randomly and it was hard to maintain the evenness of the scanning lines. For the slicing of our samples, the proper pulse energy of femtosecond laser was 10 μJ .

Another important parameter is the scanning speed. When the repetition rate of femtosecond laser is fixed, the scanning speed determines the pulse density, which indicates the energy accumulation in unit length. Figure 3(b) shows the scanning lines induced by femtosecond laser pulses with different scanning speeds under the pulse energy of 10 μJ . The slower scanning speed caused more energy accumulation, resulting in stronger damage randomly and it was hard to keep the scanning process under such random damage. In stark contrast, when the scanning speed was very fast, about 2000 $\mu\text{m/s}$ equivalent to 0.5 pulses/ μm , the voids and cracks could not be generated. According to our results, the scanning speed at 1000 $\mu\text{m/s}$ was suitable for femtosecond laser slicing in our samples.

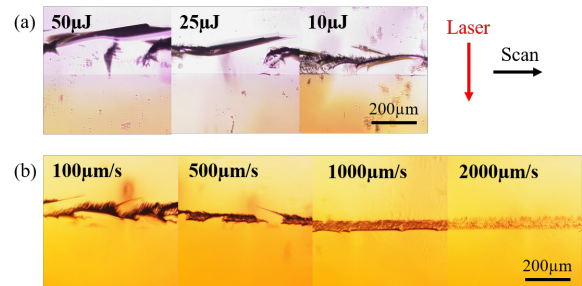


Fig. 3 The side view of the scanning lines induced by femtosecond laser pulses with (a) different pulse energy at the scanning speed of 100 $\mu\text{m/s}$ and (b) different scanning speed under the pulse energy of 10 μJ .

3.3 Separation after laser scanning

The laser pulses of 10 μJ were scanned with a pitch of 50 μm over the entire interface of the samples at the scanning speed of 1000 $\mu\text{m/s}$. The EDS mappings of N and Al on the middle of scanning line after polishing until the laser damage region were measured as shown in Fig. 4(a) and (b). The N element in the laser irradiated area decreased significantly, in contrast to the increase of Al element in the area. Fig. 4(c) and (d) showed the SEM images of the unirradiated area and the irradiated area in Fig. 4(a) respectively. The fine uneven structures in Fig. 4(d) were caused by the explosion of N_2 during AIN was decomposed to Al (s) and N_2 (g) under the irradiation of femtosecond laser.

After laser scanning, the sample was put on the Universal Testing System and a gradually increasing force was applied on the sample until it split into two pieces. The necessary force to separate the sample was 530 N as shown in Fig 5(a) and the separated samples were showed in Fig. 5(b), HVPE-AIN on the left and PVT-AIN on the right. Fig. 5(c) showed that the average maximum height R_z , the sum of the maximum peak height and the maximum pit height, of three chosen lines on the separated HVPE-AIN was less than 120 μm , which was much smaller than other conventional method. In addition, the separated PVT-AIN was polished and used to grow a new single crystal AIN by HVPE. The X-

ray topography (XRT) observation of the new HVPE-AIN was shown in Fig. 5(d). The contract in the image was due to the dislocations in the sample, which primarily existed at the interface of PVT-AIN and HVPE-AIN. In addition, compared to the previous studies [16], no apparent defect could be found in the image, which provided the evidence of the successful growth of highly pure crystal.

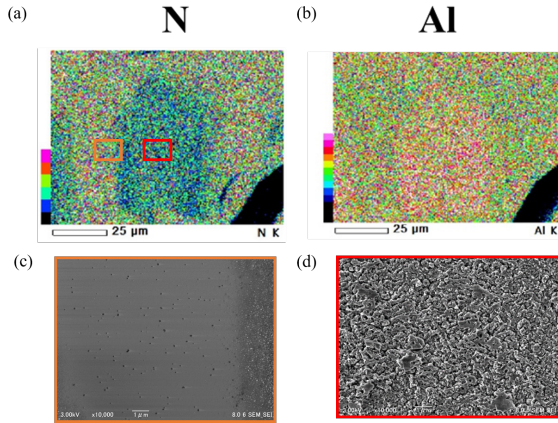


Fig. 4 The EDS mappings of N (a) and Al (b) in the laser irradiated area. The SEM image of (c) the orange rectangle area and (d) the red rectangle area in (a).

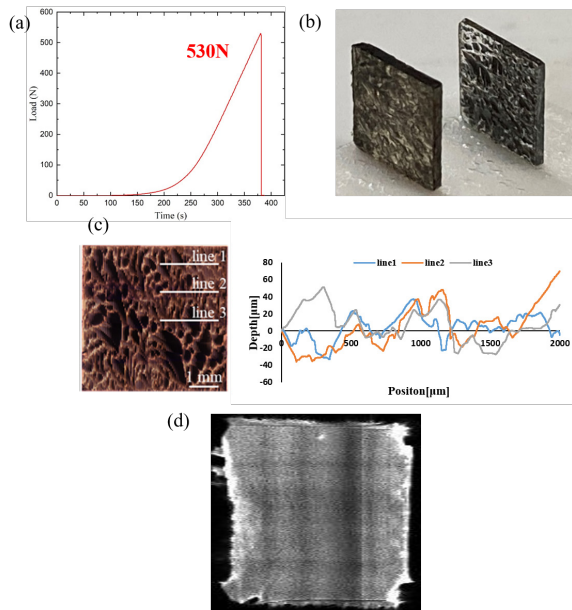


Fig. 5 (a) The force applied on the sample. (b) The completely separated sample, the left one was HVPE-AIN and the right one was PVT-AIN. (c) The surface roughness of HVPE-AIN after separation. (d) The XRT image of the new AIN crystal grown on the separated PVT-AIN after polishing by HVPE.

3.4 Double spots femtosecond laser slicing

To improve the efficiency of femtosecond laser slicing, we used a LCOS-SLM to split the laser focus into double spots. Previous studies have shown that the cracks generated by femtosecond laser multiple spots were obviously different from that generated by a single spot in some transparent materials and simultaneous irradiation had different effect on the crack generation from that of sequential irradiation [17]. In the case of our sample, the cracks generated by femtosecond laser double spots were showed in Fig. 6(a), in

which the distance between the double spots was 30 μm . When single crystal AIN was irradiated by a femtosecond laser from the c plane [0001], the cracks extended in the m plane [1100] and a plane [1120]. However, the propagation velocities of the elastic wave of both directions calculated based on the material parameters [18] were the same, that meant the cracks generation should be the same in the two directions. Therefore, the most possible reason for the different lengths of crack A and crack B in Fig. 6(a) was the effect between the two close spots. Fig. 6(b) showed the crack generation of simultaneous irradiation and sequential irradiation when the distance between the double spots was changed. Crack A was elongated obviously when the distance between the double spots was close to 30 μm under simultaneous irradiation while it was rarely changed under sequential irradiation. These results substantiated our hypothesis.

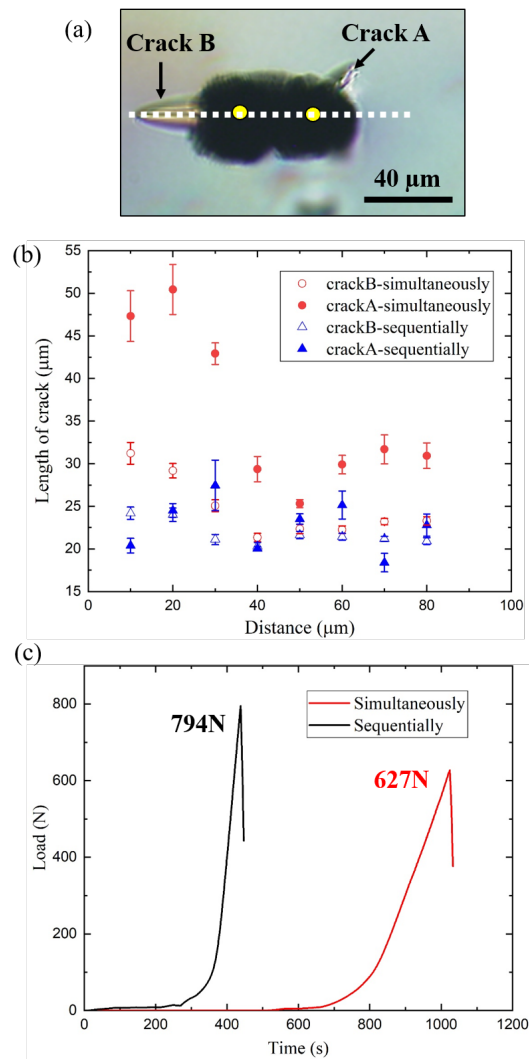


Fig. 6 The cracks generated by femtosecond laser double spots. (b) The lengths of the two kind of cracks as a function of the distance between the double spots by simultaneous irradiation and sequential irradiation. (c) The forces applied on the sample after double spots femtosecond laser slicing of simultaneous irradiation and sequential irradiation.

Based on the experimental results, we sliced the samples by femtosecond laser double spots and after scanned through the whole interface, the samples were separated by the same Universal Testing System. The forces applied on the samples were shown in Fig. 6(c), the necessary force for simultaneous irradiation was 627 N and that for sequential irradiation was 794 N. Since simultaneous irradiation had a greater effect on crack elongation than sequential irradiation did, the interface of the sample exposed to simultaneous irradiation exhibited more cracks under the same laser pulse condition and required less force to be separated.

4. Conclusion

We have demonstrated that the single crystal AlN layer grown by Hydride Vapor Phase Epitaxy could be successfully sliced off from the AlN substrate generated by Physical Vapor Transport by focusing a femtosecond laser at the interface. The kerf-loss for the femtosecond laser slicing was much smaller than conventional slicing method. The separated PVT-AlN substrate could also be reused to grow a new highly pure single crystal AlN with few defects by HVPE after polishing. The multiple spots femtosecond laser slicing was also investigated to improve the efficiency.

References

- [1] M. Feneberg, R. A. R. Leute, B. Neuschl, and K. Thonke: *Phys. Rev. B*, 82, (2010) 075208.
- [2] R. Rounds, B. Sarkar, A. Klump, C. Hartmann, T. Nagashima, R. Kirste, A. Franke, M. Bickermann, Y. Kumagai, and Z. Sitar: *Appl. Phys. Express*, 11, (2018) 071001.
- [3] Y. Taniyasu, M. Kasu, and T. Makimoto: *Nature*, 441, (2006) 325.
- [4] M. Bickermann, B. M. Epelbaum, O. Filip, P. Heimann, S. Nagata, and A. Winnacker: *Phys. Status Solidi C*, 7, (2010) 21.
- [5] A. Khan, K. Balakrishnan, and T. Katona: *Nat. Photonics*, 2, (2008) 77.
- [6] P. Reddy, M. Hayden Breckenridge, Q. Guo, A. Klump, D. Khachariya, S. Pavlidis, W. Mecouch, S. Mita, B. Moody, J. Tweedie, R. Kirste, E. Kohn, R. Collazo, and Z. Sitar: *Appl. Phys. Lett.*, 116, (2020) 081101.
- [7] R. Kirste, Q. Guo, J. H. Dycus, A. Franke, S. Mita, B. Sarkar, P. Reddy, J. M. LeBeau, R. Collazo, and Z. Sitar: *Appl. Phys. Express*, 11, (2018) 082101.
- [8] H. Hirayama, T. Yatabe, N. Noguchi, T. Ohashi and N. Kamata: *Phys. Status Solidi C*, 5, (2008) 2969.
- [9] Y. Kumagai, Y. Kubota, T. Nagashima, T. Kinoshita, R. Dalmau, R. Schlessner, B. Moody, J. Xie, H. Murakami, A. Koutitu, and Z. Sitar: *Appl. Phys. Express*, 5, (2012) 055504.
- [10] E. Kim, Y. Shimotsuma, M. Sakakura, and K. Miura: *Opt. Mater. Express*, 7, (2017) 2450.
- [11] V. V. Temnov, K. Sokolowski-Tinten, P. Zhou, A. El-Khamhawy, and D. von der Linde: *Phys. Rev. Lett.*, 97, (2006) 237403.
- [12] H. R. Reiss: *Phys. Rev. Lett.*, 29, (1972) 1129.
- [13] B. Poumellec, M. Lancry, A. Chahid-Er-raji and P. G. Kazansky: *Opt. Mater. Express*, 1, (2011) 766.
- [14] E. N. Glezer and E. Mazur: *Appl. Phys. Lett.*, 71, (1997) 882.
- [15] C. W. Smelser, S. J. Mihailov, and D. Grobner: *Opt. Express*, 13, (2005) 5377.
- [16] R. Dalmau, J. Britt, B. Moody, and R. Schlessner: *ECS Trans.*, 92, (2019) 113.
- [17] M. Sakakura, Y. Ishiguro, N. Fukuda, Y. Shimotsuma, and K. Miura: *Opt. Express*, 21, (2013) 26921.
- [18] I. Vurgaftman and J. R. Meyer: *J. Appl. Phys.*, 94, (2003) 3675.

(Received: June 15, 2023, Accepted: January 17, 2024)